Advances in Water Resources 156 (2021) 104027

Contents lists available at ScienceDirect

Advances in Water Resources

journal homepage: www.elsevier.com/locate/advwatres

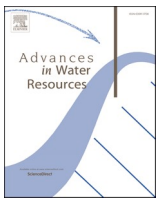

The extended generalized radial flow model and effective conductivity for truncated power law variograms

Sebastian Müller [*,a,b], Falk Heße [a,b], Sabine Attinger [a,b], Alraune Zech [c,a]

[a] Department of Computational Hydrosystems, UFZ – Helmholtz Centre for Environmental Research, Leipzig, Germany
[b] Institute of Earth and Environmental Sciences, University Potsdam, Potsdam, Germany
[c] Department of Earth Sciences, Utrecht University, Utrecht, The Netherlands

ARTICLE INFO

Keywords:
eGRF
Groundwater
Heterogeneity
Groundwater flow equation
Pumping test

ABSTRACT

Pumping tests are established for characterizing spatial average properties of aquifers. At the same time, they are promising tools to identify heterogeneity characteristics such as log-conductivity variance and correlation scales. We present the extended Generalized Radial Flow Model (eGRF) which combines the characterization of well flow in fractal geometry with an upscaled conductivity for pumping tests in heterogeneous media. We show that the eGRF is a generalization of previously solutions, such as that of Barker, Butler and Neuman. We derive effective conductivities for uniform and well flow conditions in heterogeneous log-normal media with a truncated power law correlation structure through the upscaling procedure Coarse Graining. The radial-dependent effective conductivity for well flow reflects the gradual change of heterogeneity impact on average pumping test drawdowns. We then combine upscaled conductivities with the eGRF model to determine the effective pumping test solution. We provide a proof of concept by comparing theoretical upscaling results with Monte Carlo well flow simulations in heterogeneous fractal fields. The eGRF and upscaling results are implemented and made freely available as python code for transport simulation as well as pumping test analysis.

1. Introduction

Due to their cost efficiency, pumping tests are widely-used to hydraulically characterize subsurface. Drawdowns at observation wells are fitted to analytical expression such as *Thiem's solution* (Thiem, 1906) to estimate the mean conductivity from steady-state drawdowns, or *Theis' solution* (Theis, 1935) for estimating the mean hydraulic conductivity and mean storativity from transient drawdowns. Despite their long history, pumping tests continue to evolve and new improvements are developed (Renard, 2005). However, common analyzing techniques assume a single mean conductivity to be representative for the entire aquifer domain under investigation. Consequently, their results cannot represent spatial heterogeneities, which are known to be an important feature.

For many sediments, field observations show that log-conductivity is approximately normal distributed (Gelhar, 1993; Rubin, 2003). Thus, spatial heterogeneities are modelled as log-normal random fields, characterized by the mean value and a covariance function to account for spatially correlated variability. Here, the characteristic length scale is a crucial parameter given that heterogeneity is present from pore to regional scales (Dagan, 1986).

Indelman and Abramovich (1994) showed that pumping tests in heterogeneous media cannot be interpreted by simple averaging strategies, least a homogeneous K. Representative mean values differ depending on the distance to the pumping well (Sánchez-Vila et al., 2006). An effective description of hydraulic conductivity K_{eff} is required, which reproduces the effect of heterogeneity on pumping as function of the aquifer statistics and boundary conditions. The nature of convergent flow further leads to an radially-symmetric form of the effective conductivity $K_{\text{eff}}(r)$ (Neuman et al., 2004; Schneider and Attinger, 2008). Based on a explicit effective conductivity $K_{\text{eff}}(r)$ derived through upscaling, Zech et al. (2012) proposed extensions to Thiem's and Zech et al. (2016) to Theis' formula to characterize well flow in heterogeneous aquifers. These extensions allow estimating the parameters of Gaussian fields like the mean, variance and correlation length from pumping test observations (Zech et al., 2015a).

Well flow in fractured media is even more complex since such media shows self-similarity and behaves like fractals (Bonnet et al., 2001). Diagnostic plots (Renard et al., 2009) are powerful tools to identify if pumping test observations reveal fractal behavior and consequently, if

* Corresponding author at: Department of Computational Hydrosystems, UFZ – Helmholtz Centre for Environmental Research, Leipzig, Germany.
E-mail address: sebastian.mueller@ufz.de (S. Müller).

https://doi.org/10.1016/j.advwatres.2021.104027
Received 4 February 2021; Received in revised form 25 August 2021; Accepted 2 September 2021
Available online 7 September 2021

interpretation requires to consider a non-integer dimension. However, quantitative approaches for interpreting pumping tests in heterogeneous media are still limited at best to a single correlation scale and cannot be used for an analysis of fractal properties, such as the fractal flow dimension (Barker, 1988; Borgne et al., 2004).

The *Generalized Radial Flow* (GRF) model of Barker (1988) represents an early example for an interpretative model of pumping tests in fractured media. This work was recently extended with regard to: (i) skin effect (Chang and Yeh, 2011); (ii) synthetic flow systems (Bowman et al., 2013); (iii) non-Darcian radial flow (Liu et al., 2016); (iv) generalized Forchheimer radial flow (Liu et al., 2017); and (v) generalized radial transport (Mamud, 2019). However, all these extensions are restricted to a constant value for transmissivity and storativity for the whole domain, which hampers their use to infer heterogeneous properties.

To account for the impact of heterogeneity, Butler (1988) introduced a simple approach which combines near- and far-field influences in an effective solution for the drawdown of the pumping test. Avci and Sahin (2014) generalized this concept further by modelling multiple concentric zones around the pumping well. Both approaches provide effective solutions for the drawdown but do not connect to, and therefore do not facilitate any inference of the heterogeneous properties of the conductivity field. Neuman et al. (2004) and subsequently Zech et al. (2012, 2015a) addressed this problem and extended the approach by connecting the characteristic of the heterogeneous properties of the conductivity field to the resulting drawdown. But to this day, all these approaches neither account for heterogeneous fields with fractal covariance functions nor provide a general solver for the radial symmetric groundwater flow equation. Thus, numerical tools for pumping test analysis with these methods are lacking.

We address the present shortcomings by developing an *extended GRF* (eGRF) model, which combines both aforementioned developments. The eGRF model is able to account for spatial heterogeneities, including fractal representations, using an efficient and stable numerical solver for the effective head solution of the drawdown. We demonstrate the capabilities of the eGRF model using a generalized version of the Truncated Power Law (TPL) Variogram (Di Federico and Neuman, 1997). We derive an effective, well-flow adapted conductivity field for the TPL covariance function using the upscaling procedure Coarse Graining (Attinger, 2003), in a well-flow adapted methodology (Schneider and Attinger, 2008; Zech and Attinger, 2016). In combination with the eGRF, we are able to calculate the effective drawdown solution. We demonstrate the validity of this approach by comparing the analytical method with Monte Carlo simulations of pumping tests in random fractal conductivity fields. We further make all software public available as open-source Python packages.

The course of the paper is the following: we outline the used methods such as the GRF model, the heterogeneity representation and the fundamentals on power-law variograms used to describe a fractal conductivity field. Next follows the result section where we derive the extended Generalized Radial Flow model and demonstrate how it acts as a solver for other effective solutions, previously reported in the literature. We demonstrate the upscaling procedure Coarse Graining for TPL variograms, both for uniform and well flow with particular emphasis on the effective head solution for a TPL variogram making use of the eGRF. Eventually we discuss Monte Carlo simulations that demonstrate the validity of our eGRF model for a pumping test in a heterogeneous, fractal conductivity field in two dimensions. The full mathematical derivations of the theoretical results are presented in the *Supporting Information (SI)*. We close with a summary and conclusions.

2. Methods & foundations

2.1. Generalized radial flow model

Barker (1988) introduced the generalized radial flow (GRF) model to characterize hydraulic tests in fractal geometry by the partial differential equation

$$\frac{1}{r^{d-1}}\cdot\frac{\partial}{\partial r}\left(r^{d-1}\cdot T\cdot\frac{\partial h}{\partial r}\right)=S\frac{\partial h}{\partial t} \quad , \tag{1}$$

where $h(r,t)$ is the hydraulic head as a function of the radial distance r from the well, S is the storativity, T is the transmissivity and d is the arbitrary flow dimension. The model is completed by specifying the initial condition $h(r,\ t=0)=0$, the outer boundary condition $h(r=r_{\inf},t)=0$ and the pumping condition $\lim_{r\to r_w}\oint_{B_{rw}(0)}T\cdot\nabla h\,d\sigma=-Q$ which can be rewritten in terms of $\lim_{r\to r_w}r^{d-1}\cdot\frac{\partial h}{\partial r}(r,t)=\frac{-Q}{T\cdot\alpha_d}$, where $\alpha_d=2\sqrt{\pi}^{d}\cdot\Gamma\left(\frac{d}{2}\right)^{-1}$ is the surface of the unit sphere, $r_{\inf}$ represents the aquifer dimension and r_w is the radius of the well. Further assumptions are an infinitely small well ($r_w=0$) and an infinitely big aquifer ($r_{\inf}=\infty$).

We interpret transmissivity T and storativity S as dependent on the flow dimension d, which can be calculated according to $S=S_s\cdot b^{3-d}$ and $T=K\cdot b^{3-d}$. S_s is the storage term and K the conductivity. b is the extent of the aquifer as described in Barker (1988). For integer cases of d the following interpretations hold: (i) $d=1$: b is the square root of the cross-section area and T is an integrated quantity like in 2D; (ii) $d=2$: T and S coincide with the classical meaning of storativity and transmissivity; (iii) $d=3$: the term b^{3-d} vanishes and $S=S_s$ and $T=K$. While T and S represent local constant parameter of the domain in the GRF model, we stick to the definition of T through K for the adaption to a radial dependent quantity representative for the well flow behaviour observed during pumping.

For constant values of S and T, Eq. (1) is solved by

$$h(r,t)=\frac{Qr^{2-d}}{4\sqrt{\pi}^{d}\cdot T}\Gamma\left[\frac{d}{2}-1,\frac{Sr^2}{4Tt}\right] \quad . \tag{2}$$

Here $\Gamma[s,x]$ is the incomplete Gamma function (Abramowitz et al., 1972).

2.2. Log-normal conductivity and representative averages

For the application part of this study, we model the heterogeneous hydraulic conductivity as a spatial random function following a log-normal distribution:

$$\mathrm{pdf}_K\left(x;\mu,\sigma^2\right)=\frac{1}{x\sqrt{2\pi\sigma^2}}\exp\left(-\frac{(\ln x-\mu)^2}{2\sigma^2}\right) \tag{3}$$

The parameters μ and σ^2 are the mean and variance of the underlying normal distribution of $\ln(K)\sim\mathcal{N}(\mu,\sigma^2)$.

When considering flow through log-normal conductivity, representative averages have been determined for particular flow situations. By representative hydraulic conductivity we mean a single parameter describing the average behavior of groundwater flow within an aquifer at a given scale and flow condition. A detailed review on the subject is eg. provided by Sánchez-Vila et al. (2006).

Of particular interest for us are two special cases:

- Uniform flow through isotropic, stationary media in a d-dimensional unbounded domain. The effective conductivity which describes a response of a medium to these boundary conditions is commonly described by the effective conductivity of Matheron (1967):

$$K_{\mathrm{efu}}=K_{\mathrm{G}}\cdot\exp\left(\left(\frac{1}{2}-\frac{1}{d}\right)\sigma^2\right) \quad , \tag{4}$$

  with the geometric mean $K_{\mathrm{G}}=\exp\mu$ and log-conductivity variance σ^2. Note that K_{efu} is not fully exact since it actually depends on the correlation function as shown by Stepanyants and Teodorovich

(2003), but provides a reasonable approximation.

- Radially convergent flow does not have a unique constant representative value (Indelman and Abramovich, 1994), but its asymptotic behaviour is known, depending on the assigned boundary condition (BC) at the well:

$$r\to 0: \qquad K_{\text{well}} = \begin{cases} K_{\text{H}} = K_{\text{G}}\exp\left(-\frac{1}{2}\sigma^2\right) & \text{for constant flux BC} \\ K_{\text{A}} = K_{\text{G}}\exp\left(\frac{1}{2}\sigma^2\right) & \text{for constant head BC} \end{cases} \tag{5}$$

$$r\to\infty: \qquad K_{\text{efu}} \tag{6}$$

While constant flux BC at the well are typical for studies considering 2D flow and transmissivity, i.e. well flow at larger scales, small scale pumping tests require adoption to 3D flow where a constant head BC is more realistic (Indelman et al., 1996; Indelman and Dagan, 2004). The representative conductivity in the far field refers to that of uniform flow (Eq. (4)) given that the flow there is not further impacted by the gradients at the well.

2.3. Truncated power law (TPL) variograms

2.3.1. Definition and background

Power law variograms are used in hydrogeology to account for a continuous increase in log-conductivity variance with growing domain size, which is typical for fractal media:

$$\gamma(r) = C_0 \cdot r^{2H} \quad \text{for} \quad 0 < H < 1 \quad , \tag{7}$$

where r characterizes the two-point Euclidean distance. C_0 describes the intensity of variation and H is the Hurst coefficient.

Di Federico and Neuman (1997) showed that power law variograms $\gamma(r)$ can be constructed through a superposition of classic, non-fractal variograms like the Gaussian or exponential variogram functions $\tilde{\gamma}(r, \lambda)$. This superposition is done using a weighted integral over the length scales λ:

$$\gamma(r) = \int_0^\infty \tilde{\gamma}(r,\lambda)\frac{\mathrm{d}\lambda}{\lambda} \quad . \tag{8}$$

The modes $\tilde{\gamma}(r, \lambda)$ are the classical variogram functions at each scale λ with a scale-dependent variance of $\sigma^2(\lambda) = C \cdot \lambda^{2H}$. Such fractal behaviour is typical for fractured geological media (Neuman and Di Federico, 2003; Heße et al., 2014).

Di Federico and Neuman (1997) used the integral representation in Eq. (8) to introduce an upper and lower truncation, reflecting the upper (fine size) and lower scales (resolution) of a real-world, subsurface system. Let ℓ_u and ℓ_l be these upper and lower bounds, respectively. For the sake of brevity, we assume $\ell_l = 0$ in the following. Consequently, the TPL variograms with Gaussian (γ^g) and exponential (γ^e) modes were given by Di Federico and Neuman (1997) as follows:

$$\gamma^g_{\ell_u}(r) = \frac{C\cdot\ell_u^{2H}}{2H}\cdot\left(1-\exp\left(-\frac{r^2}{\ell_u^2}\right)+\left(\left(\frac{r}{\ell_u}\right)^2\right)^H\cdot\Gamma\left[1-H,\left(\frac{r}{\ell_u}\right)^2\right]\right) \tag{9}$$

$$\gamma^e_{\ell_u}(r) = \frac{C\cdot\ell_u^{2H}}{2H}\cdot\left(1-\exp\left(-\frac{r}{\ell_u}\right)+\left(\frac{r}{\ell_u}\right)^{2H}\cdot\Gamma\left[1-2H,\frac{r}{\ell_u}\right]\right) \tag{10}$$

where $\Gamma[s, x]$ is the incomplete Gamma function (Abramowitz et al., 1972). Here, the Gaussian variogram is defined according to the auto-correlation function $\rho^g(r) = \exp\left(-\frac{r^2}{\lambda^2}\right)$ and the exponential variogram through $\rho^e(r) = \exp\left(-\frac{r}{\lambda}\right)$.

2.3.2. The stable TPL variogram

We use the stable model $\rho^s(r)$ (Wackernagel, 2003) to unify and simplify the given TPL variograms. A joint generalization of the Gaussian and exponential auto-correlation function is provided by:

$$\rho^s(r) = \exp\left(-\left(\frac{r}{\lambda}\right)^\alpha\right) \quad \text{for} \quad 0 < \alpha \le 2 \tag{11}$$

The roughness parameter $0 < \alpha \le 2$ covers the transition from the uncorrelated nugget model ($\alpha = 0$), the rough exponential model ($\alpha = 1$) up to the smooth Gaussian model ($\alpha = 2$).

Applying the stable model as modes of the TPL variogram in Eq. (8) results in the auto-correlation function of the stable TPL model

$$\rho^s_{\ell_u}(r) = \frac{2H}{\alpha}\cdot E_{1+\frac{2H}{\alpha}}\left[\left(\frac{r}{\ell_u}\right)^\alpha\right] \quad , \tag{12}$$

where $E_z[\cdot]$ is the exponential integral function (Abramowitz et al., 1972). The resulting stable TPL variogram is given by

$$\gamma^s_{\ell_u}(r) = \sigma^2_{\ell_u}\cdot\left(1-\frac{2H}{\alpha}\cdot E_{1+\frac{2H}{\alpha}}\left[\left(\frac{r}{\ell_u}\right)^\alpha\right]\right) \quad , \tag{13}$$

with variance $\sigma^2_{\ell_u} = \frac{C\cdot\ell_u^{2H}}{2H}$. The stable variogram (13) results in the truncated Gaussian (Eq. (9)) for $\alpha = 2$ and in the truncated exponential (Eq. (10)) for $\alpha = 1$.

In order for the TPL variogram (13) to converge to a power law as in Eq. (7), it has to provide a finite limit for the case of $\ell_u\to\infty$ (Di Federico and Neuman, 1997). Thus, the Hurst coefficient has to meet the condition

$$0 < H < \frac{\alpha}{2} \quad . \tag{14}$$

The Hurst coefficient ultimately controls the roughness of the corresponding field, since it determines the slope of the variogram at the origin. The TPL model is thereby able to reproduce the same spectrum of variograms as the Matérn model (Wackernagel, 2003), which is outlined in detail in the *SI*.

3. Results

3.1. The extended generalized radial flow model

3.1.1. Derivation

We extend the GRF model to account for radially dependent transmissivity $T(r)$ and storativity $S(r)$ making use of a step function approximation. Note that the radial dependency is not assumed for the underlying aquifer characteristics, but relate to the way a pumping test filters transmissivity and storativity. Thus, $T(r)$ and $S(r)$ reflect upscaled quantities, not the local ones. A similar procedure was presented by Avci and Sahin (2014) for a fixed number of concentric zones in 2D, which in turn was build on the findings of Butler (1988). The characteristic differential equation of the eGRF as extension of Eq. (1) reads:

$$\frac{1}{r^{n-1}}\cdot\frac{\partial}{\partial r}\left(r^{n-1}\cdot T(r)\cdot\frac{\partial h}{\partial r}\right) = S(r)\frac{\partial h}{\partial t} \tag{15}$$

We treat transmissivity and storativity as radial symmetric step functions:

$$T(r) = \begin{cases} T_0 & r\in R_0 \\ \vdots & \\ T_N & r\in R_N \end{cases} \qquad S(r) = \begin{cases} S_0 & r\in R_0 \\ \vdots & \\ S_N & r\in R_N \end{cases} \quad , \tag{16}$$

with T and S being constant on concentric circles around the point of origin given by $R_i = [r_i, r_{i+1})$ with $r_0 = r_w$ and $r_{N+1} = r_{\text{inf}}$.

Adapting a continuous radially-dependent transmissivity, as derived

for the TPL structure later (Eq. (22)), to the radially-symmetric step functions is achieved by making use of the harmonic average over each ring R_i. The harmonic mean of a radial symmetric function $f(r)$ over a concentric segment $R = \{x \in \mathbb{R}^d \,|\, r_0 < |x| < r_1\}$ in d dimensions is given by:

$$f_R^H = \left(\frac{d}{r_1^d - r_0^d} \int_{r_0}^{r_1} r^{d-1} f(r)^{-1} \, dr \right)^{-1} \quad . \tag{17}$$

More details on the radial harmonic mean is given in the *SI*.

Examples of the function approximations for a radially-dependent transmissivity $T(r)$ are displayed in Fig. 1 for two forms of an effective conductivity with different underlying variograms.

The hydraulic head as solution of Eqs. (15) with (16) is a piece-wise function $h_i := h|_{R_i}$ which has to fulfil conditions along the ring boundaries for $i = 0, \ldots, (N-1)$:

$$h_i(r_{i+1}, t) = h_{i+1}(r_{i+1}, t) \tag{18}$$

$$\frac{T_i}{T_{i+1}} \cdot \frac{\partial h_i}{\partial r}(r_{i+1}, t) = \frac{\partial h_{i+1}}{\partial r}(r_{i+1}, t) \quad . \tag{19}$$

The first equation is a continuity condition and the second one ensures mass conservation.

To the best of our knowledge, no analytical solution of the hydraulic head $h(r,t)$ of Eq. (15) exists. Instead, we apply the Laplace transformation to derive an equation system which can be solved by applying a penta-diagonal matrix solver as presented by Askar and Karawia (2015) and implemented by Müller (2019, 2020b). The result is then transformed back into the time domain by the algorithm of Stehfest (1970). A detailed derivation, including the full set of equations is provided in the *SI*. The whole workflow is implemented and made available as an open-source Python package named `AnaFlow` (Müller, 2020a).

3.1.2. Application of eGRF

The eGRF can be applied to arbitrary, radial conductivity functions $K(r)$ reflecting the averaging effect of pumping tests on conductivity. Examples are the extended Theis solution in 2D and 3D of Zech et al. (2016) derived from the effective representations found in Schneider and Attinger (2008), Zech et al. (2012), the apparent transmissivity of Neuman et al. (2004) as well as the transmissivity for a concentric zone aquifer of Avci and Sahin (2014), which is an extension to the two-zone aquifer described by Butler (1988). A visualization is provided in Fig. 2. (A) shows the solution of Barker (1988) for a finite domain. (B) represents the solution of Butler (1988) incorporating a separate transmissivity at the well. (C) coincides with the finding of Avci and Sahin (2014) for a finite domain. (D) is the transient solution for the apparent transmissivity presented by Neuman et al. (2004). (E) shows the effective solution for transient pumping test in heterogeneous aquifers following a Gaussian variogram derived by Schneider and Attinger (2008) which is in line with the derivations of Zech et al. (2016). (F) is an extension of (E) incorporating anisotropy in 3D (Zech et al., 2012) under the Dupuit-Forchheimer assumption to solve the depth averaged groundwater flow equation in 2D. The results match the calculations of Zech et al. (2016). All solutions share the same far-field behavior, meaning the fluctuations near the pumping well do not influence the drawdown at a sufficient distance. The solutions (D) and (E) behave very similar, which confirms, that these two approaches, to characterize effective drawdowns in heterogeneous media, result in almost the same type-curves. The solution shown in (E) was used by Müller et al. (2021) to identify parameters of aquifer heterogeneity from actual pumping test observations.

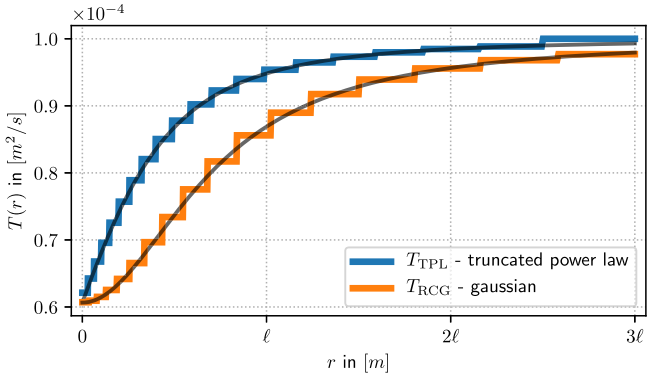

Fig. 1. Approximation as step function of radial depending transmissivity $T(r)$ for the effective well flow transmissivity using a TPL variogram $T_{\mathrm{TPL}}(r)$ (defined later in Eq. (22), $d = 2$, $H = 0.5$, $\sigma^2_{\ell_u} = 1$, $\ell_u = 5m$) and for a Gaussian variogram $T_{\mathrm{RCG}}(r)$ from Schneider and Attinger (2008) ($\sigma^2 = 1$, $\ell = 5m$).

3.2. Upscaling of TPL conductivity with coarse graining

3.2.1. Effective conductivity for uniform groundwater flow

We determine the effective conductivity for a log-normal conductivity with TPL variogram for uniform flow considering a finite filter length in the upscaling process. The *Coarse Graining* method provides a framework to analyze the groundwater flow through random conductivity fields for filtering up to a length scale λ. Following the lines of Attinger (2003), we focus on the Gaussian case of stable TPL, setting $\alpha = 2$ in Eq. (13). This choice can be justified by the often-reported insensitivity of groundwater flow to the roughness of the conductivity field (Riva and Willmann, 2009; Heße et al., 2015) and that roughness is not solely controlled by α but also H. A detailed explanation and derivation is provided in the *SI*.

The scale-dependent mean conductivity for uniform flow at the filter scale λ is given by:

$$K_{\mathrm{TPL}}^{\mathrm{uni}}(\lambda) = K_{\mathrm{G}} \cdot \exp\left(\frac{\sigma_u^2}{2} - \frac{\sigma_u^2}{d} \left(1 - \left(1 + \left(\frac{\lambda}{2\ell_u} \right)^2 \right)^{-\frac{d}{2}} \cdot \phi_d^H \left(\frac{\lambda}{2\ell_u} \right) \right) \right) \tag{20}$$

$$\phi_d^H(z) := \frac{2H}{d+2H} \cdot {}_2F_1\left[\frac{d}{2}, 1, \frac{d}{2} + H + 1, \frac{1}{1+z^2} \right] \to \begin{cases} 1 & (z \to 0) \\ \dfrac{2H}{d+2H} & (z \to \infty) \end{cases} \tag{21}$$

where K_{G} is the geometric mean, σ_u^2 is the log-conductivity variance, d denotes the dimension, H is the Hurst coefficient, ℓ_u is the upper truncation length, and ${}_2F_1$ is the ordinary hyper-geometric function (Abramowitz et al., 1972).

The result for the mean value of log-normal conductivity with a TPL variogram when filtering under uniform flow conditions (Eq. (20)) is an extension of the findings of Attinger (2003), which focused on a Gaussian variogram. The difference is solely expressed in the correction factor ϕ_d^H (Eq. (21)), which incorporates the effect of the Hurst coefficient H.

3.2.2. Effective conductivity for radially convergent flow

We apply the upscaling procedure *Radial Coarse Graining* to determine the effective mean conductivity for a well flow setting. Note, that this effective mean conductivity is neither the equivalent nor the apparent quantity (according to the classification given in Sánchez-Vila et al. (2006)), but is a quantity reproducing observed well flow when solving the flow equation with it.

Following Schneider and Attinger (2008) and Zech and Attinger (2016), we adapt the Coarse Graining procedure to radially convergent flow by substituting the filter length scale λ with the distance to the well

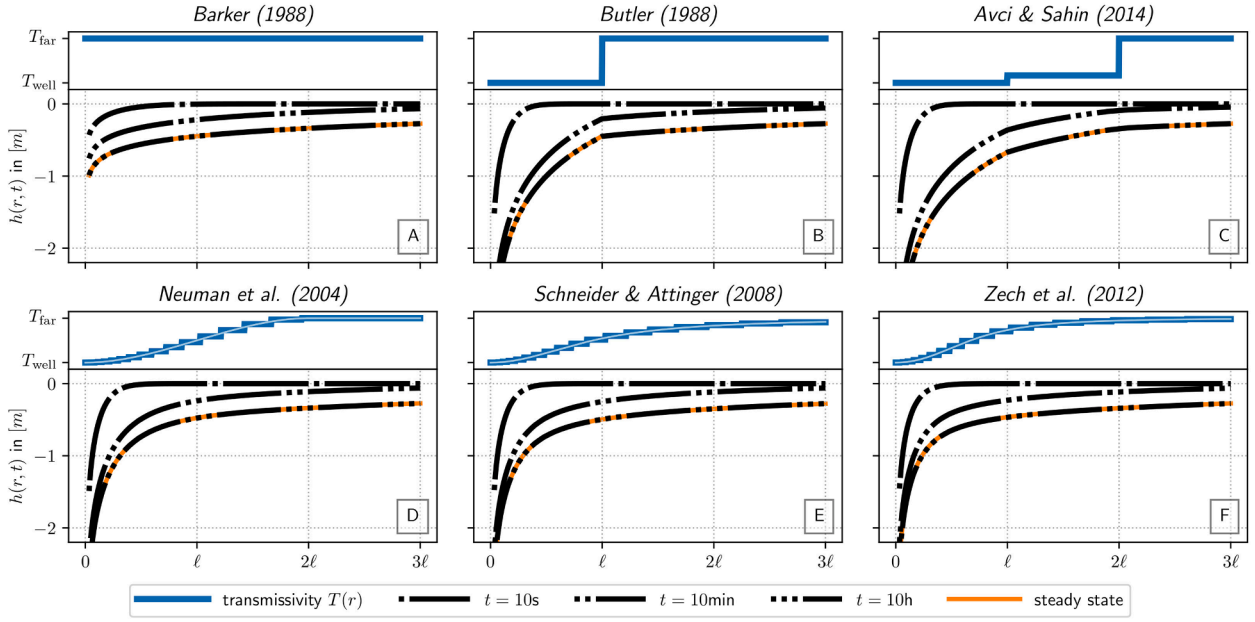

Fig. 2. Comparison of transient drawdowns for different transmissivity distributions from literature. The subplot on top shows the underlying transmissivity distribution with the two boundary values $T_{well} = 2 \times 10^{-5}\frac{m^2}{s}$ and $T_{far} = 10^{-4}\frac{m^2}{s}$ and the plot beneath shows the resulting drawdown for three time-steps derived with the eGRF model beside the analytic steady state solution in orange to demonstrate correct convergence. All solutions are derived setting a finite boundary condition $r_{inf} = 50m$ and $d = 2$ in Eq. (15). (For interpretation of the references to colour in this figure legend, the reader is referred to the web version of this article.)

r. Having a variable filter length r instead of a constant represents the non-uniform averaging behaviour of flow during pumping. The distance-dependent, effective conductivity for well flow reads:

$$K_{TPL}(r) = K_{efu} \cdot \exp\left(\chi \cdot \left(1 + \left(\frac{\xi r}{\ell_u} \right)^2 \right)^{-\frac{d}{2}} \cdot \phi_d^H \left(\frac{\xi r}{\ell_u} \right) \right) \tag{22}$$

Here K_{efu} denotes the dimension-dependent, effective conductivity for uniform flow (Eq. (4)) representative for flow far from the pumping well. χ is a short notation for the ratio $\chi = \ln \frac{K_{well}}{K_{efu}}$, where K_{well} is the effective conductivity at the pumping well, depending on the boundary condition (Eq. (5)). It simplifies to $\chi_H = \ln \frac{K_H}{K_{efu}} = \left(\frac{1}{d} - 1 \right) \sigma_u^2$ and $\chi_A = \ln \frac{K_A}{K_{efu}} = \frac{\sigma_u^2}{d}$, respectively. ξ is a proportionality factor, determined as $\xi \approx 2$ by Zech et al. (2012). $\phi_d^H(z)$ is defined in Eq. (21). $K_{TPL}(r)$ in Eq. (22) is based on the assumption of isotropy. However, it can be easily extended to a solution in $d = 3$ dimensions with vertical anisotropy following the lines of Zech et al. (2015a). The specific solution is provided in the *SI*.

The radially-symmetric effective conductivity $K_{TPL}(r)$ represents the way a pumping test radially filters the non-symmetric heterogeneity of the underlying regular log-normal field (Eq. (3)) with TPL variogram (Eq. (7)). Fig. 3 shows the shape of the effective conductivity as function of the dimensionless ratio of radial distance to correlation scale ℓ_u. It displays the transition between the two representative conductivities for well flow: K_{efu} in the far field (dimension dependent) and K_H at the well (assuming the constant flux BC here). The specifics of this transition are a function of the correlation structure and its defining parameters.

The effective conductivity $K_{TPL}(r)$ is in line with effective representations of conductivity for well tests such as of Neuman et al. (2004); Schneider and Attinger (2008), Zech et al. (2012), Zech et al. (2015a), Zech and Attinger (2016), Zech et al. (2016). They all provide effective transmissivity or conductivity distributions that act as a transition between the harmonic mean at the pumping well and the effective far field value.

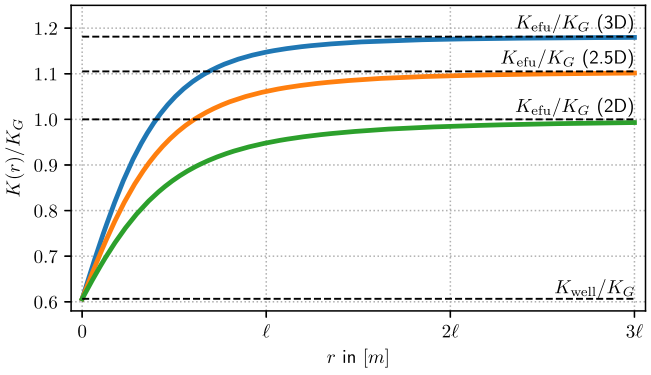

Fig. 3. Effective well flow conductivity $K_{TPL}(r)$ for truncated power law (TPL) variogram in two, three and fractal dimension ($d = 2.5$) according to Eq. (22) using $\sigma_u^2 = 1$ and $H = 0.5$. Values are normalized (divided) by the geometric mean K_G. Lines indicate asymptotic values near the well ($K_{well} = K_H$) and in the far field (K_{efu}).

3.2.3. *Effective head solution for TPL variograms*

The representative mean hydraulic head for a pumping test results from solving the groundwater flow equation in radial coordinates (Eq. (15)) with $K_{TPL}(r)$ along the lines of Zech et al. (2012, 2016). A closed-form, analytical expression cannot be determined. Instead, we provide semi-analytical type curves making use of the eGRF (Section 3.1).

We solve the flow equation with the eGRF inserting the effective TPL-conductivity (Eq. (22)) for $T(r)$. The resulting effective head drawdown $h_{TPL}(r,t)$ can be interpreted as an average behaviour representing the well flow through a heterogeneous aquifers with a log-normal conductivity distribution following a TPL variogram. A visual impression is provided in Fig. 4 for a certain choice of aquifer statistical parameters. Head values have been determined numerically making use of `AnaFlow`.

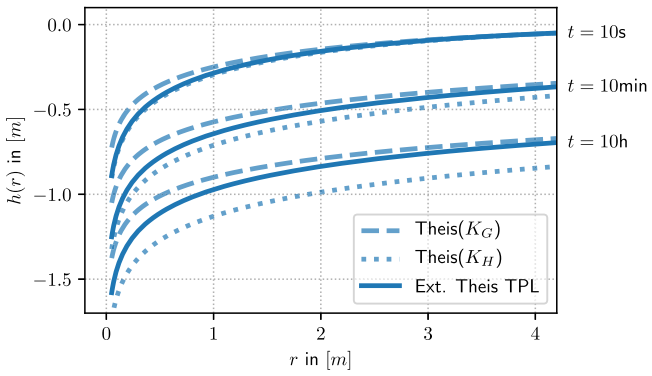

Fig. 4. Effective mean drawdown of a pumping tests in heterogeneous log-normal conductivity with TPL variogram as solution of the groundwater equation making use of the effective well flow TPL-transmissivity $T_{\mathrm{TPL}}(r)$ (Eq. 22) at three points in time. It is compared to Theis solution with a uniform conductivity for the two representative values of well flow: $T_{\mathrm{well}} = T_{\mathrm{H}}$ (in 2D) near the well and T_{G} for the far field. (Parameters: $d = 2$, $H = 0.5$ $\sigma_u^2 = 0.5$, $\ell_u = 10\mathrm{m}$, $S = 10^{-4}$, $T_{\mathrm{G}} = 10^{-4}\frac{\mathrm{m}}{\mathrm{s}}$, $Q = -10^{-4}\frac{\mathrm{m}^3}{\mathrm{s}}$).

3.3. Proof of concept with Monte Carlo simulations

We performed numerical pumping tests simulations in random conductivity as virtual measurements to demonstrate the viability of our method. The average pumping test drawdown $h_{\mathrm{ens}}(r,t)$ for an ensemble of log-normal transmissivity fields with a TPL variogram provides the representative behaviour of well flow in heterogeneous aquifers. The ensemble average drawdown $h_{\mathrm{ens}}(r,t)$ is independent from the (semi-) analytical upscaling results $h_{\mathrm{TPL}}(r,t)$. We compare both results to prove the validity of $h_{\mathrm{TPL}}(r,t)$ as semi-analytical generalization of effective pumping test behaviour.

First, we generate ensembles of 1000 log-normal random transmissivity fields (Eq. (3)) with a TPL variogram (Eq. (9)) using the Python-package `GSTools` (Müller and Schüler, 2020; Heße et al., 2014). One realization is shown in Fig. 5. We cover various parameter combinations with variances of $\sigma^2 = 1$ and 2.25; upper length scale of correlation $\ell = 10$ m and 20 m and Hurst coefficient $H = 0.5$ and 0.9.

Pumping tests are simulated using the finite-element software OpenGeoSys through the Python API `ogs5py` (Müller et al., 2020). We use a process adapted 2D radially symmetric numerical mesh. It has a

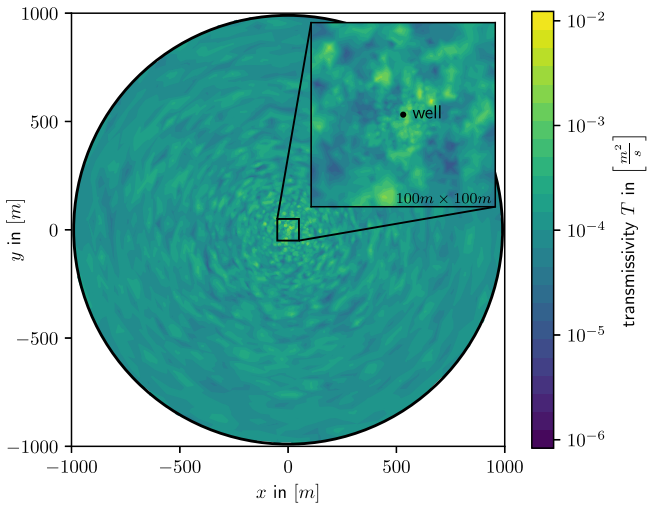

Fig. 5. Generated transmissivity field following a TPL variogram with parameters $T_{\mathrm{G}} = 10^{-4}\frac{\mathrm{m}^2}{\mathrm{s}}$, $\sigma^2 = 1.0$, $\ell = 10\mathrm{m}$ and $H = 0.5$. Note that the transmissivity field does not contain symmetry effects. The smoothing of the field towards the outer boundary is due to the decreasing resolution of the radial mesh.

diameter of 2000m to avoid boundary effects, 64 angular subdivisions and 100 radial units, with resolution decreasing with distance to the pumping well. We applied a constant flux boundary condition at the well with a constant pumping rate of $Q_w = -10^{-4}$ m^3/s. Technical details are further outlined in the *SI*.

The simulated drawdown of each heterogeneous transmissivity realizations is averaged over the angle to gain a solely radial depending head. Ensemble means $h_{\mathrm{ens}}(r,t)$ for each set of statistical parameters is achieved through averaging over the $N = 1000$ individual numerical pumping tests.

Fig. 6 shows the calculated ensemble mean for the parameter set P0 with $S = 10^{-4}$, $T_{\mathrm{G}} = 10^{-4}\frac{\mathrm{m}^2}{\mathrm{s}}$, $\sigma^2 = 1.0$, $\ell = 10\mathrm{m}$ and $H = 0.5$ in comparison to the effective drawdown $h_{\mathrm{TPL}}(r,t)$ for the same parameters with a relative error of 2.56%. Results of all other ensembles are provided in the *SI* along with information about relative errors between ensemble means and effective heads. Interested readers can generate their own ensemble making use of the provided workflow (Müller and Zech, 2021).

The agreement of the ensemble mean $h_{\mathrm{ens}}(r,t)$ and the effective drawdown $h_{\mathrm{TPL}}(r,t)$ in Fig. 6 (the same holds for all other ensembles, see *SI*) provides evidence that $T_{\mathrm{TPL}}(r)$ represents the effective transmissivity for pumping test in this particular heterogeneous structure. Thus the average drawdown behaviour of pumping tests can be predicted based on the transmissivity statistics using $h_{\mathrm{TPL}}(r,t)$.

4. Summary and conclusions

We presented the extended General Radial Flow model (eGRF), which combines the mathematical characterization of well flow in arbitrary (fractal) dimensions and an effective description of conductivity for pumping tests in heterogeneous log-normal fields. The non-uniform effective conductivity accounts for the radial filtering effect of well flow on aquifer heterogeneity. Results are implemented in an efficient and stable numerical solver to compute the effective head drawdown from the radial flow equation. The eGRF extends the advantage of the General Radial Flow model (Barker, 1988) of non-integer dimensions of the flow system to heterogeneous fractal aquifers. We show that the eGRF acts as general solver for non-uniform transmissivity descriptions of pumping tests, such as that of Butler (1988), Neuman et al. (2004), Avci and Sahin (2014) or Zech et al. (2016).

We further derive effective conductivities for uniform flow and for pumping tests in heterogeneous aquifers with a log-normal conductivity distribution and a truncated power law (TPL) correlation structure. This conceptualization of the heterogeneity represents fractal aquifers which exhibit structures with more then one length scale. We used the upscaling procedure Coarse Graining to derive effective conductivity descriptions as a function of the TPL-heterogeneity input parameters mean, log- conductivity variance, (upper) correlation scale and Hurst-coefficient. We present an analytical expression for mean conductivity which represent average behaviour under uniform flow conditions at a particular filter length scale. Results are extended to radial convergent flow conditions leading to an effective (upscaled) conductivity function depending on the radial distance and aquifer statistics. Making use of the presented eGRF, we determine the effective drawdown behaviour, i.e. the hydraulic head as function of radial distance and TPL-heterogeneity parameters.

We show that upscaling results are indeed representing well flow in log-normal media with a TPL correlation structure by performing Monte Carlo flow simulations. We generated ensembles of random fields with various parameter combinations and performed numerical pumping tests. These independent ensemble simulations are fully in line with the mean drawdown predicted by the TPL-effective head from the eGRF.

The presented results lead us to the following conclusions:

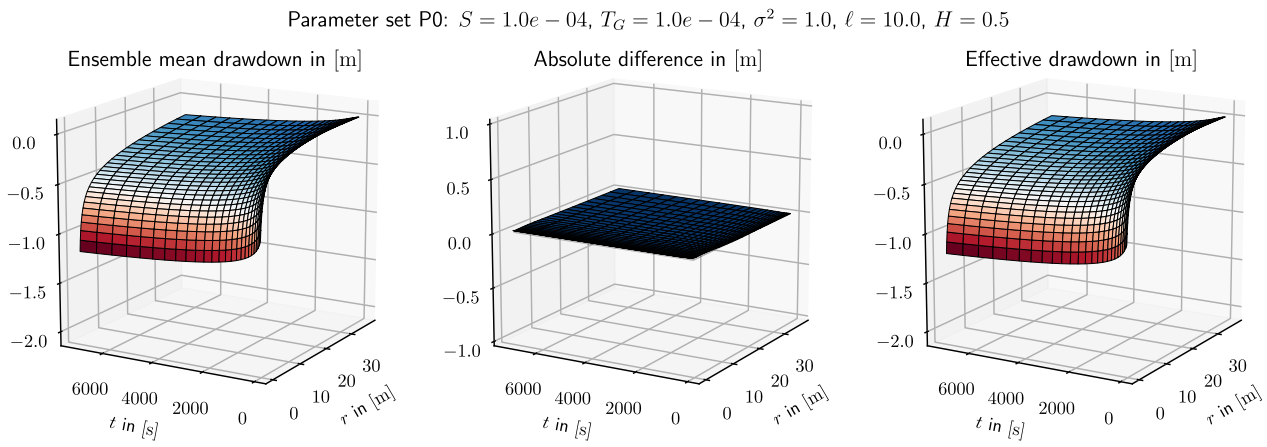

Fig. 6. Comparison of the ensemble mean drawdown $h_{\text{ens}}(r,t)$ (left) with the effective head solution $h_{\text{TPL}}(r,t)$ (right) for parameter set P0. The vanishing absolute difference between both (middle) shows, that they perfectly agree.

- The eGRF can be used to calculate pumping test drawdowns for an arbitrary form of (upscaled) radial transmissivity $T(r)$. This opens the opportunity to generate type-curves for effective transient drawdowns in heterogeneous media.
- Well flow in heterogeneous fields with a truncated power law correlation structure can be effectively described in the average with an analytical expression for the conductivity as function of the radial distance to the well and the statistical field parameters.
- The methodology can be used for inverse aquifer characterization. Comparing observed drawdowns to eGRF drawdowns of effective TPL-transmissivity allows estimating mean storativity, mean transmissivity, log-transmissivity variance, (upper) correlation scale and Hurst-coefficient.

The results presented herein are a sound foundation for verifying the applicability of the method using real data from heterogeneous aquifers. We anticipate and plan further studies on e.g. (i) the significance of fractal flow dimensions d in interaction with effective transmissivity distributions, (ii) the analysis of actual field pumping tests in fractured media, (iii) analyzing the influence of radial varying storativity.

While fractals are well established for describing fractured media with its heterogeneities at multiple scales, it is still under debate if porous media shows such behaviour, at least at the scale of interest here. Although some authors report on self-similar porous media with heterogeneities at increasing scales, (e.g. Desbarats and Bachu, 1994; Molz et al., 2004; Neuman et al., 2008), many studies build on the (miss-) interpretation of the data reported by Gelhar et al. (1992) along the universal scaling of macrodispersivity, which is actually not supported by reliable field data (Zech et al., 2015b; 2018). Given that the matter is still debated, we leave it to the user if he considers it legitimate to use a fractal model in porous media.

The presented novel methodology, including open-source software implementations (Müller and Zech, 2021), does not only provide a workflow to describe pumping test in heterogeneous aquifers of arbitrary flow dimension and fractal heterogeneity structure, but allows quantifying it. Thus, we can infer fractal heterogeneity characteristics from pumping test drawdowns.

Code Availability

Software packages with solution implementations and scripts for reproducing figures and ensemble simulations are given at:

- `GeoStat-Examples/extended-GRF-model` (Müller and Zech, 2021): workflow to reproduce results of this paper
- `AnaFlow` (Müller, 2020a): implementation of the eGRF model, the effective solution h_{TPL} and the effective transmissivity T_{TPL}
- `pentapy` (Müller, 2019): pentadiagonal matrix solver used for the eGRF solution in Laplace space
- `GSTools` (Müller and Schüler, 2020): TPL variograms and random field generation

CRediT authorship contribution statement

Sebastian Müller: Conceptualization, Methodology, Software, Validation, Formal analysis, Writing – original draft, Visualization. **Falk Heße:** Writing – original draft, Writing – review & editing. **Sabine Attinger:** Supervision. **Alraune Zech:** Conceptualization, Validation, Writing – review & editing, Supervision.

Declaration of Competing Interest

The authors declare that they have no known competing financial interests or personal relationships that could have appeared to influence the work reported in this paper.

Acknowledgements

Sebastian Müller was funded by the German Federal Environmental Foundation via grant number 20016/432. The authors are thankful to the editors, the anonymous reviewers and Aldo Fiori for their constructive comments which helped to improve the manuscript.

Supplementary material

Supplementary material associated with this article can be found, in the online version, at 10.1016/j.advwatres.2021.104027.

References

Abramowitz, M., Stegun, I.A., et al., 1972. Handbook of Mathematical Functions. Dover Publications, New York.
Askar, S.S., Karawia, A.A., 2015. On solving pentadiagonal linear systems via transformations. Math. Probl. Eng. 2015, 232456. https://doi.org/10.1155/2015/232456.
Attinger, S., 2003. Generalized coarse graining procedures for flow in porous media. Comput. Geosci. 7, 253–273. https://doi.org/10.1023/B:COMG.0000005243.73381.e3.
Avci, C.B., Sahin, A.U., 2014. Assessing radial transmissivity variation in heterogeneous aquifers using analytical techniques. Hydrol. Process. 28, 5739–5754. https://doi.org/10.1002/hyp.10064.
Barker, J.A., 1988. A generalized radial flow model for hydraulic tests in fractured rock. Water Resour. Res. 24, 1796–1804. https://doi.org/10.1029/WR024i010p01796.

Bonnet, E., Bour, O., Odling, N.E., Davy, P., Main, I., Cowie, P., Berkowitz, B., 2001. Scaling of fracture systems in geological media. Rev. Geophys. 39, 347–383. https://doi.org/10.1029/1999RG000074.

Borgne, T.L., Bour, O., Dreuzy, J.R.d., Davy, P., Touchard, F., 2004. Equivalent mean flow models for fractured aquifers: insights from a pumping tests scaling interpretation. Water Resour. Res. 40, W03512. https://doi.org/10.1029/2003WR002436.

Bowman, D.O., Roberts, R.M., Holt, R.M., 2013. Generalized radial flow in synthetic flow systems. Groundwater 51, 768–774. https://doi.org/10.1111/j.1745-6584.2012.01014.x.

Butler Jr., J., 1988. Pumping tests in nonuniform aquifers – the radially symmetric case. J. Hydrol. 101, 15–30. https://doi.org/10.1016/0022-1694(88)90025-X.

Chang, Y.C., Yeh, H.D., 2011. Skin effect in generalized radial flow model in fractured media. Geophys. J. Int. 185, 78–84. https://doi.org/10.1111/j.1365-246X.2011.04943.x.

Dagan, G., 1986. Statistical theory of groundwater flow and transport: pore to laboratory, laboratory to formation, and formation to regional scale. Water Resour. Res. 22, 120S–134S.

Desbarats, A.J., Bachu, S., 1994. Geostatistical analysis of aquifer heterogeneity from the core scale to the basin scale: a case study. Water Resour. Res. 30, 673–684. https://doi.org/10.1029/93WR02980.

Di Federico, V., Neuman, S.P., 1997. Scaling of random fields by means of truncated power variograms and associated spectra. Water Resour. Res. 33, 1075–1085. https://doi.org/10.1029/97WR00299.

Gelhar, L.W., 1993. Stochastic Subsurface Hydrology. Prentice Hall, Englewood Cliffs, N. Y.

Gelhar, L.W., Welty, C., Rehfeldt, K.R., 1992. A critical review of data on field-scale dispersion in aquifers. Water Resour. Res. 28, 1955–1974. https://doi.org/10.1029/92WR00607.

Heße, F., Prykhodko, V., Schlüter, S., Attinger, S., 2014. Generating random fields with a truncated power-law variogram: a comparison of several numerical methods. Environ. Model. Softw. 55, 32–48. https://doi.org/10.1016/j.envsoft.2014.01.013.

Heße, F., Savoy, H., Osorio-Murillo, C.A., Sege, J., Attinger, S., Rubin, Y., 2015. Characterizing the impact of roughness and connectivity features of aquifer conductivity using Bayesian inversion. J. Hydrol. 531, 73–87. https://doi.org/10.1016/j.jhydrol.2015.09.067.

Indelman, P., Abramovich, B., 1994. Nonlocal properties of nonuniform averaged flows in heterogeneous media. Water Resour. Res. 30, 3385–3393. https://doi.org/10.1029/94WR01782.

Indelman, P., Dagan, G., 2004. A note on well boundary condition for flow through heterogeneousformations. Water Resour. Res. 40, W03601. https://doi.org/10.1029/2003WR002602.

Indelman, P., Fiori, A., Dagan, G., 1996. Steady flow toward wells in heterogeneous formations: mean head and equivalent conductivity. Water Resour. Res. 32, 1975–1984. https://doi.org/10.1029/96WR00990.

Liu, M.M., Chen, Y.F., Hong, J.M., Zhou, C.B., 2016. A generalized non-Darcian radial flow model for constant rate test. Water Resour. Res. 52, 9325–9343. https://doi.org/10.1002/2016WR018963.

Liu, M.M., Chen, Y.F., Zhan, H., Hu, R., Zhou, C.B., 2017. A generalized Forchheimer radial flow model for constant-rate tests. Adv Water Resour 107, 317–325. https://doi.org/10.1016/j.advwatres.2017.07.004.

Mamud, M.L., 2019. Generalized radial transport model for interpreting convergent flow tracer tests in fractured rock. Electronic Theses and Dissertations. https://egrove.olemiss.edu/etd/1632

Matheron, G., 1967. Elements pour une theorie des milieux poreux. Maisson et Cie, Paris.

Molz, F.J., Rajaram, H., Lu, S., 2004. Stochastic fractal-based models of heterogeneity in subsurface hydrology: origins, applications, limitations, and future research questions. Rev. Geophys. 42, RG1002. https://doi.org/10.1029/2003RG000126.

Müller, S., 2019. pentapy: a Python toolbox for pentadiagonal linear systems. J. Open Source Softw. 4, 1759. https://doi.org/10.21105/joss.01759.

Müller, S., 2020. GeoStat-Framework/AnaFlow v1.0.1. Zenodo. https://doi.org/10.5281/zenodo.3738268.

Müller, S., 2020. GeoStat-Framework/pentapy v1.1.0. Zenodo. https://doi.org/10.5281/zenodo.3723583.

Müller, S., Leven, C., Dietrich, P., Attinger, S., Zech, A., 2021. How to find aquifer statistics utilizing pumping tests? Two field studies using welltestpy. Groundwater. https://doi.org/10.1111/gwat.13121.

Müller, S., Schüler, L., 2020. GeoStat-Framework/GSTools: Volatile Violet v1.2.1. Zenodo. https://doi.org/10.5281/zenodo.3751743.

Müller, S., Zech, A., 2021. GeoStat-Examples/extended-GRF-model: v1.1. Zenodo. https://doi.org/10.5281/zenodo.4772717.

Müller, S., Zech, A., Heße, F., 2020. ogs5py: a Python-API for the OpenGeoSys 5 scientific modeling package. Groundwater 59, 117–122. https://doi.org/10.1111/gwat.13017.

Neuman, S.P., Di Federico, V., 2003. Multifaceted nature of hydrogeologic scaling and its interpretation. Rev. Geophys. 41, 1014. https://doi.org/10.1029/2003RG000130.

Neuman, S.P., Guadagnini, A., Riva, M., 2004. Type-curve estimation of statistical heterogeneity. Water Resour. Res. 40, W04201. https://doi.org/10.1029/2003WR002405.

Neuman, S.P., Riva, M., Guadagnini, A., 2008. On the geostatistical characterization of hierarchical media. Water Resour. Res. 44, W02403. https://doi.org/10.1029/2007WR006228.

Renard, P., 2005. The future of hydraulic tests. Hydrogeol. J. 13, 259–262. https://doi.org/10.1007/s10040-004-0406-5.

Renard, P., Glenz, D., Mejias, M., 2009. Understanding diagnostic plots for well-test interpretation. Hydrogeol. J. 17, 589–600. https://doi.org/10.1007/s10040-008-0392-0.

Riva, M., Willmann, M., 2009. Impact of log-transmissivity variogram structure on groundwater flow and transport predictions. Adv. Water Resour. 32, 1311–1322. https://doi.org/10.1016/j.advwatres.2009.05.007.

Rubin, Y., 2003. Applied Stochastic Hydrogeology. Oxford University Press, New York.

Sánchez-Vila, X., Guadagnini, A., Carrera, J., 2006. Representative hydraulic conductivities in saturated groundwater flow. Rev. Geophys. 44, RG3002. https://doi.org/10.1029/2005RG000169.

Schneider, C.L., Attinger, S., 2008. Beyond Thiem - a new method for interpreting large scale pumping tests in heterogeneous aquifers. Water Resour. Res. 44, W04427. https://doi.org/10.1029/2007WR005898.

Stehfest, H., 1970. Numerical inversion of laplace transforms. Commun. ACM 13, 47–49. https://doi.org/10.1145/361953.361969.

Stepanyants, Y.A., Teodorovich, E.V., 2003. Effective hydraulic conductivity of a randomly heterogeneous porous medium. Water Resour. Res. 39 https://doi.org/10.1029/2001WR000366._eprint: https://agupubs.onlinelibrary.wiley.com/doi/pdf/10.1029/2001WR000366

Theis, C.V., 1935. The relation between the lowering of the piezometric surface and the rate and duration of discharge of a well using groundwater storage. Trans. Am. Geophys. Union 16, 519–524. https://doi.org/10.1029/TR016i002p00519.

Thiem, G., 1906. Hydrologische Methoden. J.M. Gebhardt, Leipzig.

Wackernagel, H., 2003. Multivariate Geostatistics: An Introduction with Applications, third ed. Springer-Verlag, Berlin Heidelberg. https://doi.org/10.1007/978-3-662-05294-5.

Zech, A., Arnold, S., Schneider, C., Attinger, S., 2015. Estimating parameters of aquifer heterogeneity using pumping tests - implications for field applications. Adv. Water Resour. 83, 137–147. https://doi.org/10.1016/j.advwatres.2015.05.021.

Zech, A., Attinger, S., 2016. Technical note: analytical drawdown solution for steady-state pumping tests in two-dimensional isotropic heterogeneous aquifers. Hydrol. Earth Syst. Sci. 20, 1655–1667. https://doi.org/10.5194/hess-20-1655-2016.

Zech, A., Attinger, S., Cvetkovic, V., Dagan, G., Dietrich, P., Fiori, A., Rubin, Y., Teutsch, G., 2015. Is unique scaling of aquifer macrodispersivity supported by field data? Water Resour. Res. 51, 7662–7679. https://doi.org/10.1002/2015WR017220.

Zech, A., D'Angelo, C., Attinger, S., Fiori, A., 2018. Revisitation of the dipole tracer test for heterogeneous porous formations. Adv. Water Resour. 115, 198–206. https://doi.org/10.1016/j.advwatres.2018.03.006.

Zech, A., Müller, S., Mai, J., Heße, F., Attinger, S., 2016. Extending theis' solution: using transient pumping tests to estimate parameters of aquifer heterogeneity. Water Resour. Res. 52, 6156–6170. https://doi.org/10.1002/2015WR018509.

Zech, A., Schneider, C.L., Attinger, S., 2012. The extended thiem's solution - including the impact of heterogeneity. Water Resour. Res. 48, W10535. https://doi.org/10.1029/2012WR011852.